SI Materials and Methods

Mice

The S196A floxed ($S196A^{fl/fl}$) mouse line was generated by Ozgene Pty Ltd (Bentley WA, Australia). The genomic sequence for the murine LXRα (Nr1h3) gene was obtained from the Ensembl Mouse Genome Server (http://www.ensembl.org/Mus_musculus/), Ensembl gene ID: ENSMUSG00000002108. The mutant fragment, located on Exon 5, contains a serine-to-alanine mutation at Ser196 introduced by site-directed mutagenesis. The point-mutant exon was delivered into an intronic site inside the targeting vector, placed in opposite orientation and thus without coding capacity (Fig. S1A). The targeting construct was electroporated into the Bruce4 C57BL/6 ES cell line. Homologous recombinant ES cell clones were identified by Southern hybridization and injected into BALB/cJ blastocysts. Male chimeric mice were obtained and crossed to C57BL/6J females to establish heterozygous germline offsprings on a pure C57BL/6 background. The germline mice were crossed to a FLP Recombinase mouse line(1) to remove the FRT flanked selectable marker cassette (Flp'd mice ($Flp^{+/+}$). $Flp^{+/+}$ mice are homozygous for FL allele containing LXRα WT exon 5 (Ex5) and LXRα S196A exon 5 of the LXRα gene in opposite orientation flanked by lox sites sensitive to Cre recombinase activity. These mice express LXRα WT but switch to LXRα S196A expression in the presence of CRE recombinase. $Flp^{+/+}$ mice were crossed with (1) a C57BL/6 homozygous Ldl receptor null ($Ldlr^{-KO}$) mouse strain, to generate a $Flp^{+/+}Ldlr^{-KO}$ strain and (2) a C57BL/6 homozygous LysMCre ($LysMCre^{+/+}$) strain to generate a $Flp^{+/+}LysMCre^{+/-}$ strain. The two resulting lines were then crossed to generate $Flp^{+/+}Ldlr^{-KO}LysMCre^{+/-}$. Cre recombinase expression under direction of the LysM promoter in $Flp^{+/+}Ldlr^{-KO}LysMCre^{+/-}$ results in the switch to LXRα S196A expression in myeloid cells, these mice ($M\text{-}S196A^{Ldlr\text{-}KO}$) were compared to littermate non- CRE expressing mice ($Flp^{+/+}Ldlr^{-KO}LysMCre^{-/-}$ or $WT^{Ldlr\text{-}KO}$) which were used as controls in our study. The Ldlr-KO and LysMCre strains were purchased from The Jackson Laboratory (stock numbers 002207 and 004781, respectively)

Animals were housed together and maintained in a pathogen-free animal facility in a 12-h light-12h dark cycle. All procedures were carried under the UK's Home Office Animals (Scientific Procedures) Act 1986.

Genotyping

Mice were genotyped by PCR analysis of ear biopsies using Jumpstart Taq DNA Polymerase (Sigma Aldrich) and the following primers: For S198A knock-in, primers R2 and WT identify the wild-type allele (642bp) and FL allele (656bp), primers R2 and SA identifly the mutant allele of LXRα S196A knock-in mice (656 bp): SA 5' GGTGTCCCCAAGGGTGTCCG wild-type 5' GGTGTCCCCAAGGGTGTCCT, R2 5' AAGCATGACCTGCACACAAG, Ldlr; oIMR0092 (mutant): 5' AATCCATCTTGTTCAATGGCCGATC, oIMR3349 (common): 5' CCATATGCATCCCCAGTCTT, oIMR3350 (wild-type): 5' GCGATGGATACACTCACTGC, LysMcre; oIMR3066 (mutant): 5'

CCCAGAAATGCCAGATTACG, oIMR3067 (common): 5' CTTGGGCTGCCAGAATTTCTC, oIMR3068 (wild-type): 5' TTACAGTCGGCCAGGCTGAC.

Diet induced atherosclerosis

Eight-week old $WT^{Ldlr\text{-}KO}$ and $M\text{-}S196A^{Ldlr\text{-}KO}$ male mice were fed ad libitum a Western diet (WD) (20% Fat, 0.15% Cholesterol; #5342 AIN-7A, Test Diet Limited, UK) for 12 weeks. Mice were fasted overnight prior to sacrifice.

Metabolic tests

Blood was sampled from saphenous vein as previously described(2). Glucose concentrations were determined in whole blood by a portable meter (Roche Diagnostics, 2 Burgess Hill, UK). Plasma insulin concentrations were determined by enzyme-linked immunoassay (#EZRMI-13K, Merck Millipore). Plasma total cholesterol and triglyceride levels (Wako Diagnostics), as well as NEFAs (Abcam), were determined by colorimetric enzymatic assay kits as per the manufacturer's recommendations.

Atherosclerosis quantification

***En face* analysis of aorta.** Mice were perfusion-fixed with phosphate-buffered paraformaldehyde (4% [wt/vol.], pH 7.2) under terminal anaesthesia. The entire aortic tree was dissected free of fat and other tissue. Aortae were stained with oil red O and mounted onto glass slides before imaging (Leica, DFC310FX) under a dissection microscope (Leica, MZ10F). Lesion area of whole aorta was analysed using Image J.

Aortic sinus. Hearts were formalin-fixed, paraffin-embedded and 5 µm aortic sinus sections were stained with stained with hematoxylin and eosin (H&E). Stained sections were scanned with NanoZoomer Digital slide scanner (Hamamatsu). Percentage atherosclerotic lesion were determined using Image J by averaging 3 sections from each mouse with 30-50 µm intervals between sections(2).

Macrophage content. Immunohistochemistry staining was performed at the UCL IQPath Laboratory using the Ventana Discovery XT instrument, using the Ventana DAB Map detection Kit (760-124). For pre-treatment Ventana Protease 1 (equivalent to pronase, 760-2018) was used. CD68 primary antibody (AbD Serotec #MCA1957), followed by Rabbit anti Mouse (#E0354 Dako). Stained sections were scanned with NanoZoomer Digital slide scanner (Hamamatsu). Macrophage content was quantified in the plaque using Image J.

Plaque complexity. Percent necrotic core was measured in H&E stained aortic roots as acellular area(3) using Image J.

Cell culture

Bone marrow derived macrophage culture. Bone Marrow-derived Macrophages (BMDM) were prepared as in(4) using L929 Conditioned Medium (LCM) as a source of M-CSF for the differentiation of the macrophages. After 6 days of differentiation, LCM-containing medium was removed, cells were washed three times in warm PBS and incubated in DMEM containing low-endotoxin (≤10 EU/mL) 1% FBS and 20 µg/mL gentamycin without any LCM before being treated with DMSO or 1 µmol/L GW3965 (Tocris) for 24 hrs. For inhibitor experiments, 5 days post-differentiation, LCM-containing medium was removed, cells washed three times with warm PBS and incubated with DMEM containing low endotoxin (≤10 EU/mL) 10% FBS and 20 µg/mL gentamycin without any LCM before being treated with DMSO or FDI-6 (#1392, Sigma) at indicated concentrations for 24 (mRNA quantification) or 48 hours (flow cytometry).

Isolation of mouse peritoneal macrophages. Peritoneal macrophages were harvested 4 days after i.p. injection of 4% thioglycolate by peritoneal lavage. Macrophages were seeded at $2x10^6$ cells/mL in RPMI and adherent macrophages were washed in PBS and harvested after 2 hours.

Jurkat culture. Jurkat cells were cultured in RPMI supplemented with 10% FBS and passaged every two days to maintain a cell concentration not exceeding $1x10^6$ cells/mL.

RAW 264.7 culture. RAW-LXRα and RAW-S198A cells expressing receptors were cultured as decribed(5).

Efferocytosis

Jurkat cells or BMDM were labeled for 1 hr with calcein AM and apoptosis was induced by UV irradiation. Apoptotic cells were added to monolayers of BMDM at a ratio of 1:1. After 30 min of co-culture, non-ingested apoptotic cells were removed, and slides fixed in 1% PFA. Images were captured (microscope: Zeiss Axio Vert.A1, camera: Zeiss Axiocam 503 mono) and ingested apoptotic cells quantified as in(6) using Image J.

Ki67 Staining by flow cytometry

Macrophages were washed with PBS before incubation with dissociation media (PBS + 10µM EDTA + 4mg/mL lidocaine + Pen/Strep) at 37°C for 15 minutes and removal from tissue culture plates by gentle scraping. Cells were stained with a Zombie™ Fixable Viability Dye (BioLegend), followed by anti-Mouse F4/80-FITC (Clone BM8, eBioscience™), then fixed and permeabilised using eBioscience™ Fixation/Permeabilisation reagents (Invitrogen). Intracellular staining with PE Mouse anti-Ki67 Set (BD Pharmingen™) was performed in eBioScience™ Permeabilisation Buffer (Invitrogen) for 30 minutes at 4°C. Samples were acquired on a BD LSR Fortessa™ X-20 (BDBioscience) using BD FACSDiva™ Software. Data was analysed using FlowJo® v10.4 (Tree Star Inc.)

Monocytosis

Blood samples were obtained by cardiac puncture. Red blood cells were lysed for 17s in distilled water, followed by a second lysis using ACK lysis buffer (Lonza). Cells were washed once in cell staining buffer, stained with Zombie^{TM} Fixable Viability Dye (BioLegend), followed by surface staining with anti-Mouse CD45-BV510 (clone 30-F11, BD Biosciences), CD11b- PerCP Cy5.5 (clone M1/70, eBioscience) and CD115-PE (clone AFS98, BioLegend). Cells were washed in cell staining buffer and resuspended in 0.5% PFA with CountBright absolute counting beads (ThermoFisher).

RNA extraction and quantification

Total RNA from was extracted with TRIzol Reagent (Invitrogen). Sample concentration and purity was determined using a NanoDrop™ 1000 Spectrophotometer and cDNA was synthesized using the qScript cDNA Synthesis Kit (Quanta). Specific genes were amplified and quantified by quantitative Real Time-PCR, using the PerfeCTa SYBR Green FastMix (Quanta) on an MX3000p system (Agilent). Primer sequences are shown in supplementary table S5. The relative amount of mRNAs was calculated using the comparative Ct method and normalized to the expression of cyclophylin(7).

Protein isolation and immunoblotting

Total cellular protein lysates (30µg) or nuclear extracts were loaded onto a 10% SDS-PAGE gel, electrophoresed and transferred onto a PVDF membrane. Membranes were probed with anti-LXRα (ab41902, Abcam), phospho-Ser196 specific rabbit polyclonal antibody (8), and anti-Hsp90 (sc-7947, Santa Cruz) overnight in 2.5% BSA, TBS, followed by incubation with anti-rabbit (PO448, Dako) or anti-mouse (NA931VS, GE Healthcare) horseradish-peroxidase-tagged antibodies. Chemiluminescence (ECL 2 Western Blotting Substrate, Pierce) was used to visualise proteins.

RNA sequencing and analysis

Total RNA was extracted using TRIzol reagent (Life technologies) and cDNA libraries were prepared using reagents and protocols supplied with the Stranded mRNA-Seq Kit (Kapa Biosystems). Briefly, poly-A tailed RNA was purified using paramagnetic oligo-dT beads from 200 nanograms of total RNA, with a RNA Integrity Number above 7.5 as determined by the Agilent Bioanalyzer (Agilent). The purified RNA was chemically fragmented and cDNA was synthesised using random primers (Kapa Biosystems). Adapter-ligated DNA library was amplified with 12 cycles of PCR and library fragment was estimated using the Agilent TapeStation 2200.Library concentration was determined

using the Qubit DNA HS assay (Life Technologies). Libraries were sequenced on an Illumina NextSeq 500, NCS v2.1.2 (Illumina) with a 43bp paired end protocol. Basecalling was done using standard Illumina parameters (RTA 2.4.11). Sequencing and pipeline analysis was performed by UCL Genomics (London, UK) and using Partek Flow software. Reads were demulitplexed using Illumina bcl2fastq v2.17 (Illumina) and aligned using STAR v2.5.0b to the mouse GRCm38/mm10 reference sequence. Transcript abundance was estimated using Illumina's RnaReadCounter tool and differential expression analysis performed with DESeq2, which uses the Benjamin-Hochberg method for multiple testing correction (FDR< 0.05). Pathway enrichment analysis was performed with the Gene Set Enrichment Analysis (GSEA) software's preranked module(9, 10) or the GSEA module in the WebGestalt (http://www.webgestalt.org) analysis toolkit. Reactome pathway analysis was performed with WebGestalt using the Benjamini-Hochberg method to adjust p values for multiple testing and FDR <0.05. Heatmaps of gene counts were done with Heatmapper Expression tool(11) (http://www1.heatmapper.ca/expression/) and Venn diagrams using a BGE tool (http://bioinformatics.psb.ugent.be/webtools/Venn/). Dot and box plot graphs were generated using Partek Flow software.

ChIP-sequencing

Immortalized bone marrow derived-macrophages (iBMDM) from LXRαβ$^{-/-}$ mice have been described(12). N-terminus 3xFLAG-tagged LXRα or LXRβwere ectopically expressed in LXR-null iBMDM using a pBabe-puro retroviral expression system as described(13). A control LXRαβ$^{-/-}$ iBMDM line was also prepared by transduction with an empty pBabe-puro vector. For genome-wide binding analysis of LXR proteins, FLAG-tagged cells were cultured in DMEM supplemented with 1% FFA-free BSA, 50nM of Zaragozic acid (Squalene Synthase inhibitor; Sigma), and 1 uM of GW3965 LXR agonist or GW2033 LXR antagonist (both kindly provided by Jon Collins, Glaxo SmithKline) for 24 h. Immortalized bone marrow derived-macrophages (12 x 10^6) were crosslinked with 2mM DSG (disuccinimidyl glutarate) for 30 min and 1% methanol-free ultrapure formaldehyde for 10 min before quenching with 2 M Glycine. Cells were lysed with RIPA buffer and, after chromatin shearing by sonication (Bioruptor Diagenode), incubated overnight with protein G magnetic Dynabeads (Invitrogen) that were previously coupled with 3 µg of anti-FLAG M2 (Sigma) antibodies according to the manufacturer's instructions. Immunoprecipitated DNA was purified using Qiagen columns. For high-throughput sequencing, ds DNA was obtained by pooling DNA from 10 independent ChIP (for FLAG-LXR sequencing). DNA was then used for library preparation and subsequent Illumina HiSeq sequencing by the Centre de Regulació Genomica (CRG, Barcelona, Spain) genomic facility.

Chomatin immunoprecipitation

ChIP experiments were performed and analysed as described(7) except cells were cross-linked with 2mM of disuccinimidyl glutarate (Thermo Scientific) for 20 min, followed by 10 min with 1% formaldehyde solution (Thermo Scientific). The antibodies employed include: LXRα (#61176, Active Motif, 10μg) and H3K27ac (ab4729, Abcam, 3μg). Oligonucleotides used are shown in Supplementary Table S6. To control for non-specific binding, an 82 base pair fragment in a gene desert in chromosome 6 using commercial oligonucleotides (#71011,ActiveMotif) was used.

Statistics

Results are expressed as mean (SEM). Comparisons within groups were made using paired Students t-tests and between groups using unpaired Students t tests or repeated measures ANOVA, as appropriate; where repeated *t-tests* were performed a Bonferroni correction was applied. P≤0.05 considered statistically significant except for RNAseq analysis where P≤0.01 was used.

References

1. Takeuchi T, et al. (2002) Flp recombinase transgenic mice of C57BL/6 strain for conditional gene targeting. *Biochem Biophys Res Commun* 293(3):953–957.
2. Gage MC, et al. (2013) Endothelium-specific insulin resistance leads to accelerated atherosclerosis in areas with disturbed flow patterns: a role for reactive oxygen species. *Atherosclerosis* 230(1):131–9.
3. Feng B, et al. (2003) Niemann-Pick C heterozygosity confers resistance to lesional necrosis and macrophage apoptosis in murine atherosclerosis. *Proc Natl Acad Sci* 100(18):10423–10428.
4. Pineda-Torra I, Gage M, de Juan A, Pello OM (2015) Isolation, Culture, and Polarization of Murine Bone Marrow-Derived and Peritoneal Macrophages. *Methods Mol Biol* 1339:101–9.
5. Torra IP, et al. (2008) Phosphorylation of liver X receptor alpha selectively regulates target gene expression in macrophages. *Mol Cell Biol* 28(8):2626–36.
6. Thorp E, et al. (2011) Shedding of the Mer Tyrosine Kinase Receptor Is Mediated by ADAM17 Protein through a Pathway Involving Reactive Oxygen Species, Protein Kinase Cζ, and p38 Mitogen- activated Protein Kinase (MAPK) *. doi:10.1074/jbc.M111.263020.
7. Pourcet B, et al. (2011) LXRα regulates macrophage arginase 1 through PU.1 and interferon regulatory factor 8. *Circ Res* 109(5):492–501.
8. Torra IP, et al. (2008) Phosphorylation of liver X receptor alpha selectively regulates target gene expression in macrophages. *Mol Cell Biol* 28(8):2626–2636.
9. Mootha VK, et al. (2003) PGC-1α-responsive genes involved in oxidative phosphorylation are coordinately downregulated in human diabetes. *Nat Genet* 34(3):267–273.

10. Subramanian A, et al. (2005) Gene set enrichment analysis: a knowledge-based approach for interpreting genome-wide expression profiles. *Proc Natl Acad Sci U S A* 102(43):15545–50.
11. Babicki S, et al. (2016) Heatmapper: web-enabled heat mapping for all. *Nucleic Acids Res* 44(W1):W147–W153.
12. Ito A, et al. (2015) LXRs link metabolism to inflammation through Abca1-dependent regulation of membrane composition and TLR signaling. *Elife* 4:e08009.
13. Chen M, Bradley MN, Beaven SW, Tontonoz P (2006) Phosphorylation of the liver X receptors. *FEBS Lett* 580(20):4835–4841.

Supplementary Figure 1

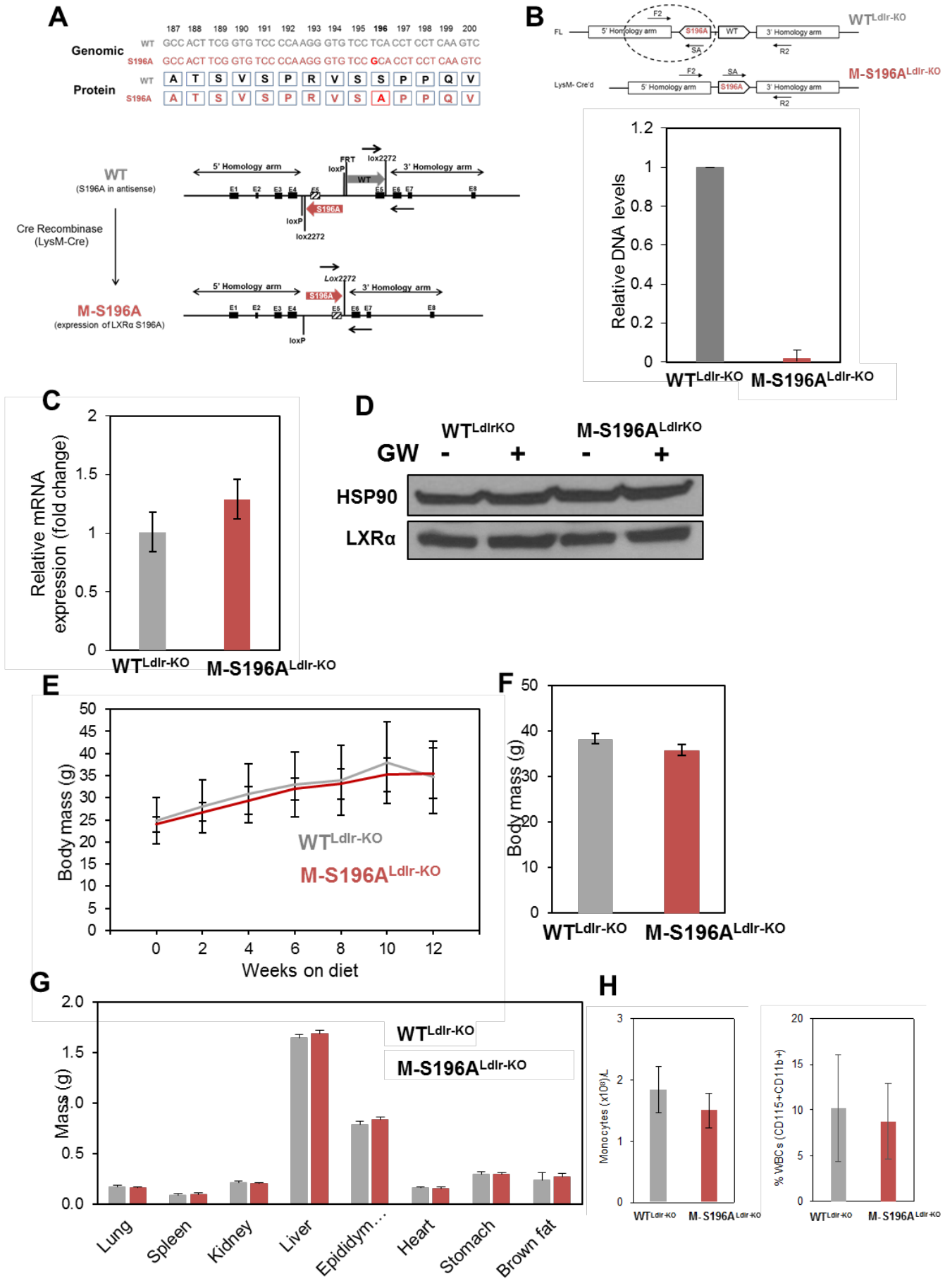

(**A**) *(Top)* WT and S196A genomic and protein sequence alignment of the murine LXRα depicting the single-site mutation at S196A. *(Bottom)* Schematic diagram illustrating the targeting construct used for the generation of M-S196A model and targeted loci. (**B**) Relative levels of $S196A^{FL/FL}$ (n=4 per group) for the quantification of cre-mediated recombination efficiency showing $M\text{-}S196A^{Ldlr\text{-}KO}$ mice express the knock-in mutation in macrophages**.** Primer pair F2-SA selectively amplifies FL allele in $S196A^{fl/fl}$ (WT). (**C**) LXRα expression in BMDMs by RT-qPCR analysis (n=3/genotype). (**D**) LXRα protein expression in BMDMs by Western blot analysis. (**E**) Growth curve (n=8-11 per group). (**F**) Terminal body mass (n >20 mice per group). (**G**) Organ mass (n=8-11 per group). (**H**) (*Left*) Number of monocytes or (*Right*) percentage of white blood cells in blood (n=3 mice per genotype).

Supplementary Figure 2

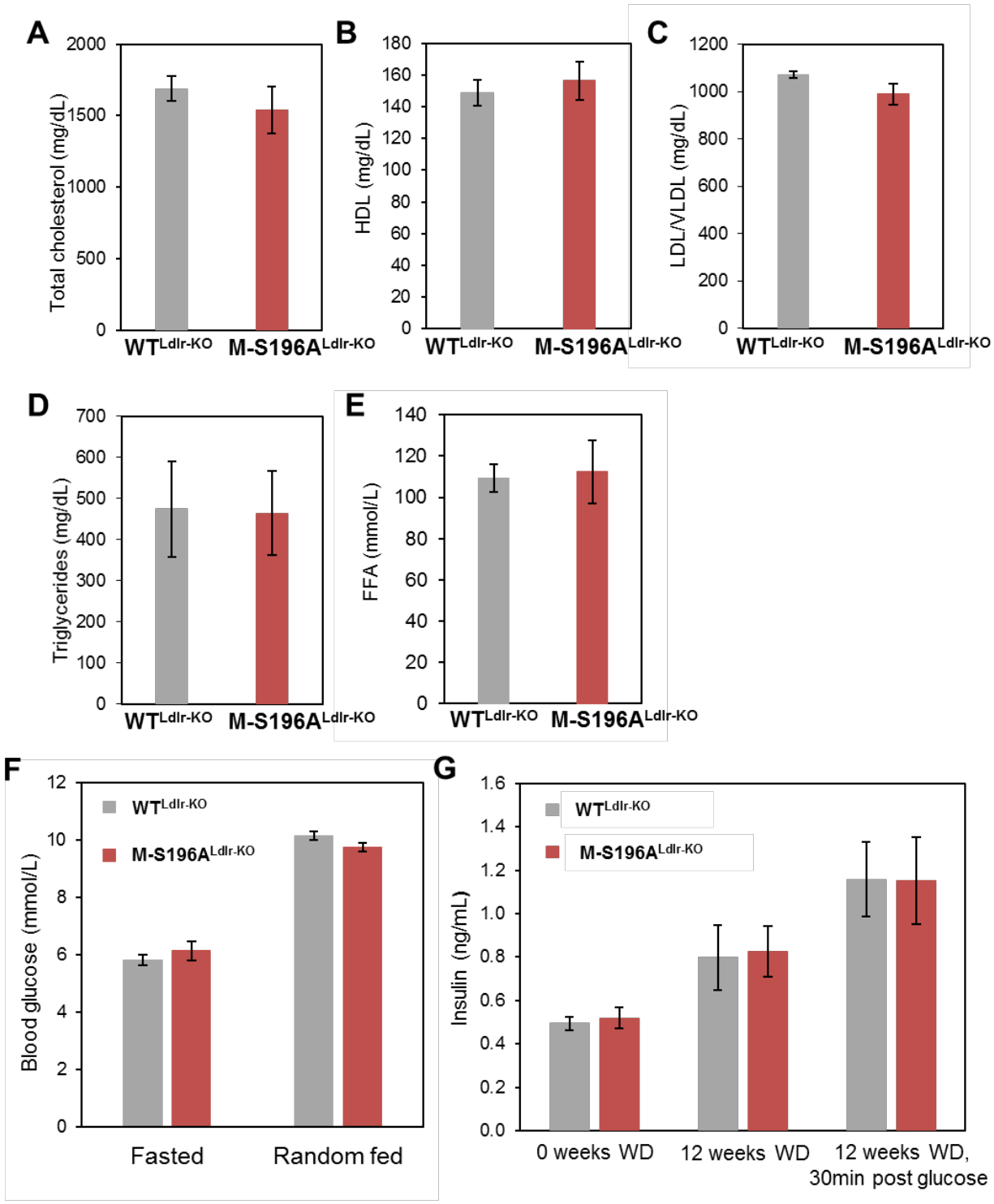

Plasma (**A**) total cholesterol, (**B**) HDL cholesterol, (**C**) LDL/VLDL cholesterol, (**D**) Triglycerides and (**E**) Free fatty acids. Blood (**F**) glucose and (**G**) insulin (n=6 -11 mice per group).

Supplementary Figure 3

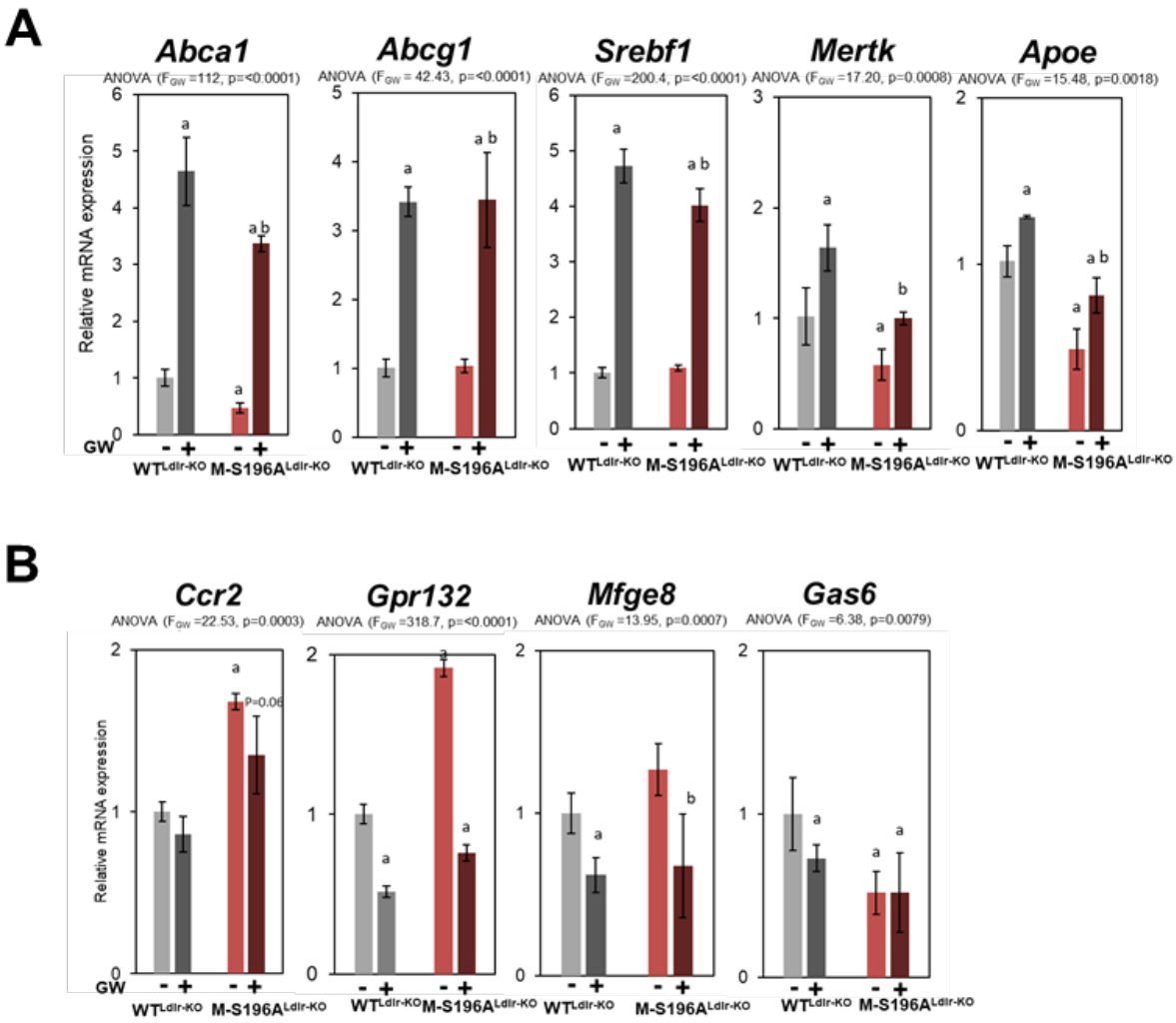

(A) RT-qPCR analysis of LXR targets in response to LXR activation by GW 3965 (GW) in WT^{LdlrKO} and $M\text{-}S196A^{LdlrKO}$ macrophages. (**B**) RT-qPCR analysis of a selection of genes with efferocytosis functions and respose to LXR activation by GW 3965 (GW) in WT^{LdlrKO} and $M\text{-}S196A^{LdlrKO}$ macrophages. Normalised data shown relative to WT^{LdlrKO} as mean ± SD, n=3, (a) compared to WT-DMSO, (b) compared to M-S196A-DMSO.

Supplementary Figure 4

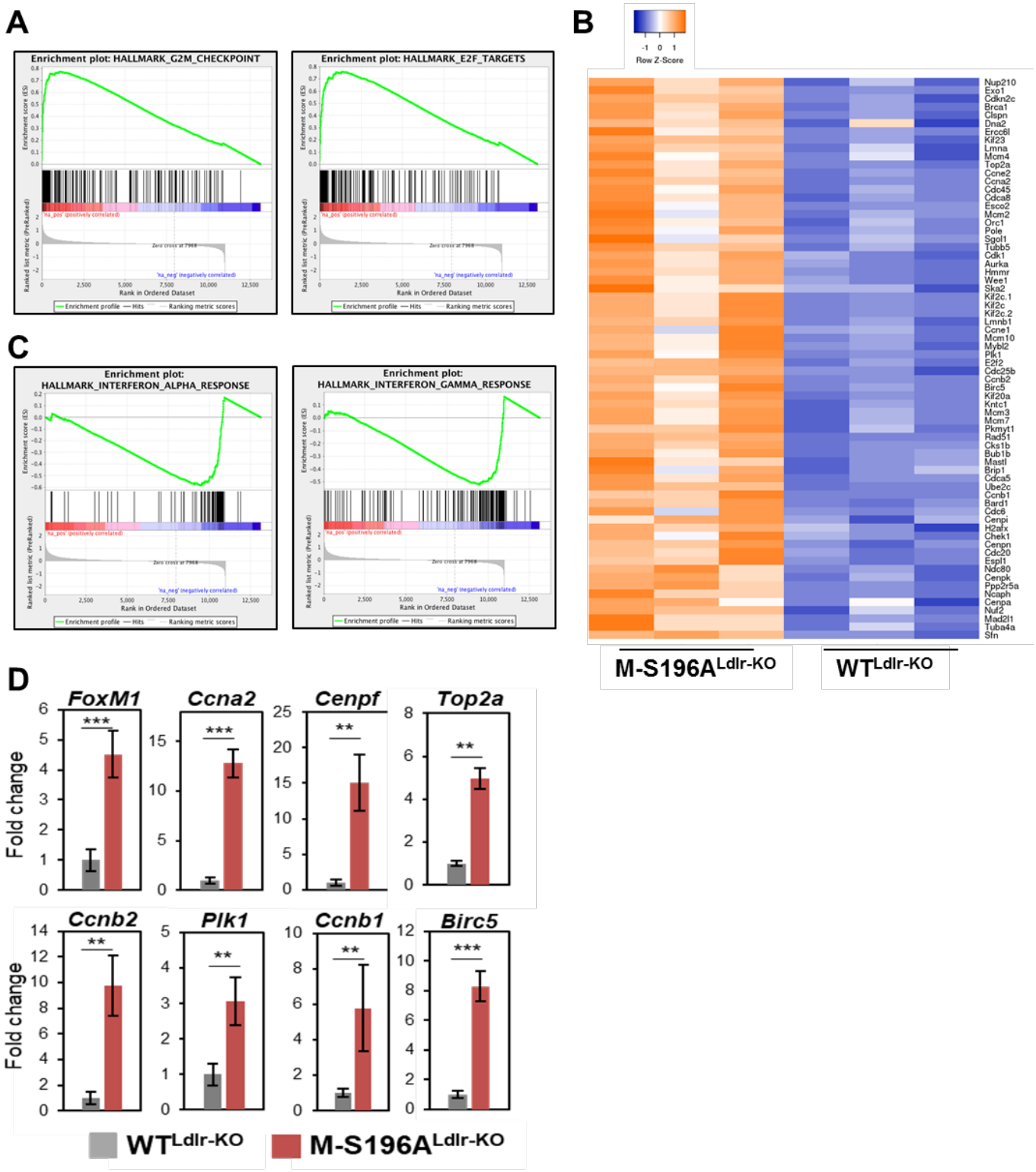

(**A**) Enrichment plots for top 2 induced Hallmark pathways in WD-fed M-S196A$^{Ldlr\text{-}KO}$ macrophages compared to WD-fed WT$^{Ldlr\text{-}KO}$. (**B**) Clustered heatmap of macrophage RNAseq gene counts of cell cycle and proliferation genes in WD-fed mice (n=3/genotype). (**C**) Enrichment plots for top 2 reduced Hallmark pathways in WD-fed M-S196A$^{Ldlr\text{-}KO}$ macrophages compared to WD-fed WT$^{Ldlr\text{-}KO}$. (**D**) RT-qPCR analysis of FoxM1 and top FoxM1 regulated targets in WD-

fed WT$^{Ldlr-KO}$ and M-S196A$^{Ldlr-KO}$ macrophages. Normalized data shown relative to WT$^{Ldlr-KO}$ (set as 1) as mean ± SEM, n=3, **p<0.01 or ***p<0.001.

Supplementary Figure 5

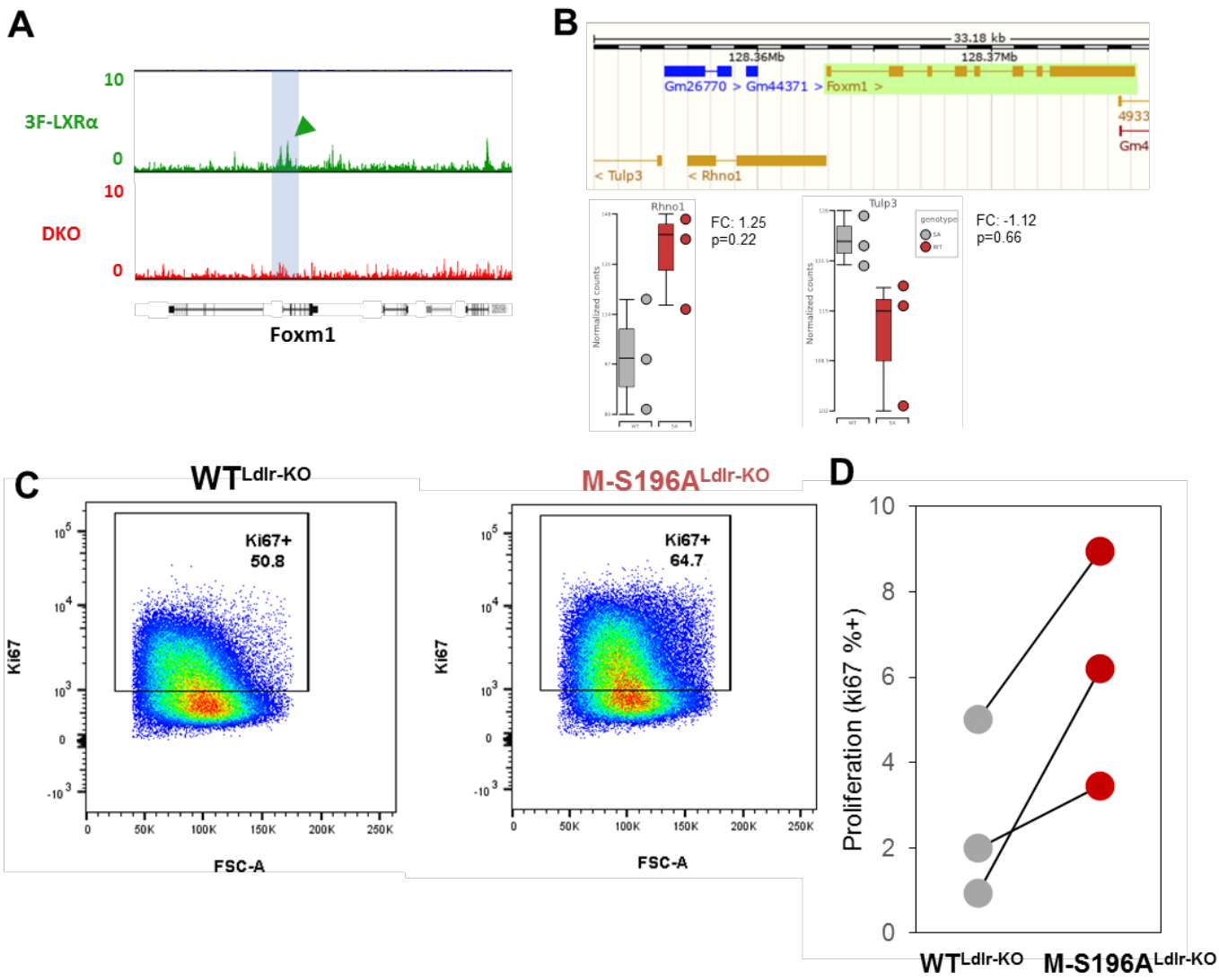

(**A**) ChIPseq LXRα track on LXR-deficient BMDMs (DKO, red tracks) or BMDMs overexpressing FLAG-tagged LXRa (green tracks) cells incubated with GW3965 ligand. Arrowheads point at identified peaks. (**B**) (Top) Screenshot depicting genes upstream of the FoxM1 locus. (Bottom) Box and dot plots of normalised gene counts for Rhno1 and Tulp3, located upstream of FoxM1. (**C**) FACS plots of Ki67 levels in WT$^{Ldlr-KO}$ and M-S196A$^{Ldlr-KO}$ macrophages. Shown is a representative experiment of 2. (**D**) Linked dot plots showing increased proliferation of M-S196A$^{Ldlr-KO}$ macrophages in three independent experiments, 1-2 mice/ genotype.

Supplementary Figure 6

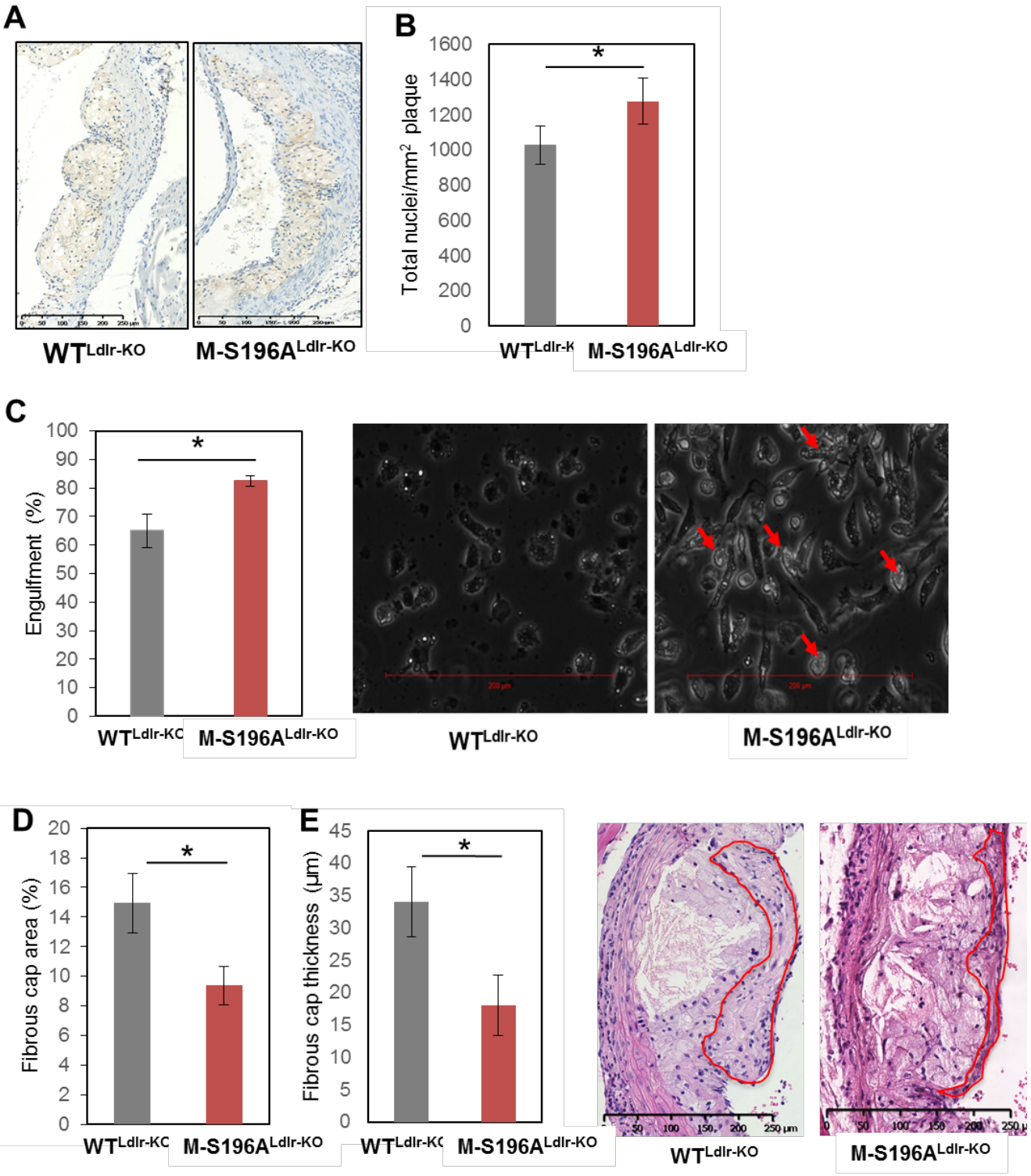

(**A**) Representative images of CD68 stained aortic root sections, scale bar at 250 µm. (**B**) Quantification of total number of nuclei per mm^2 of plaque from H&E-stained sections (n=6/ group). (**C**) (*Left*) Apoptotic macrophage (BMDMs) engulfment by $WT^{Ldlr\text{-}KO}$ or $M\text{-}S196A^{Ldlr\text{-}KO}$ macrophages (n=3/ group. (*Right*) Representative images for each genotype shown, scale bar at 200 µm. Shown is a representative experiment of 2 independent sets. (**D**) Fibrous cap area (% of total atherosclerotic lesion area) (n=6/ group) and (**E**) (*Left*) Fibrous cap thickness quantification (n=6/ group). (*Right*) Representative images of plaques with delineated fibrous caps in red, scale bar at 250µm. Data represents means ± SEM. * $p < 0.05$ relative to $WT^{Ldlr\text{-}KO}$ determined by Student's t-test.

Supplementary Figure 7

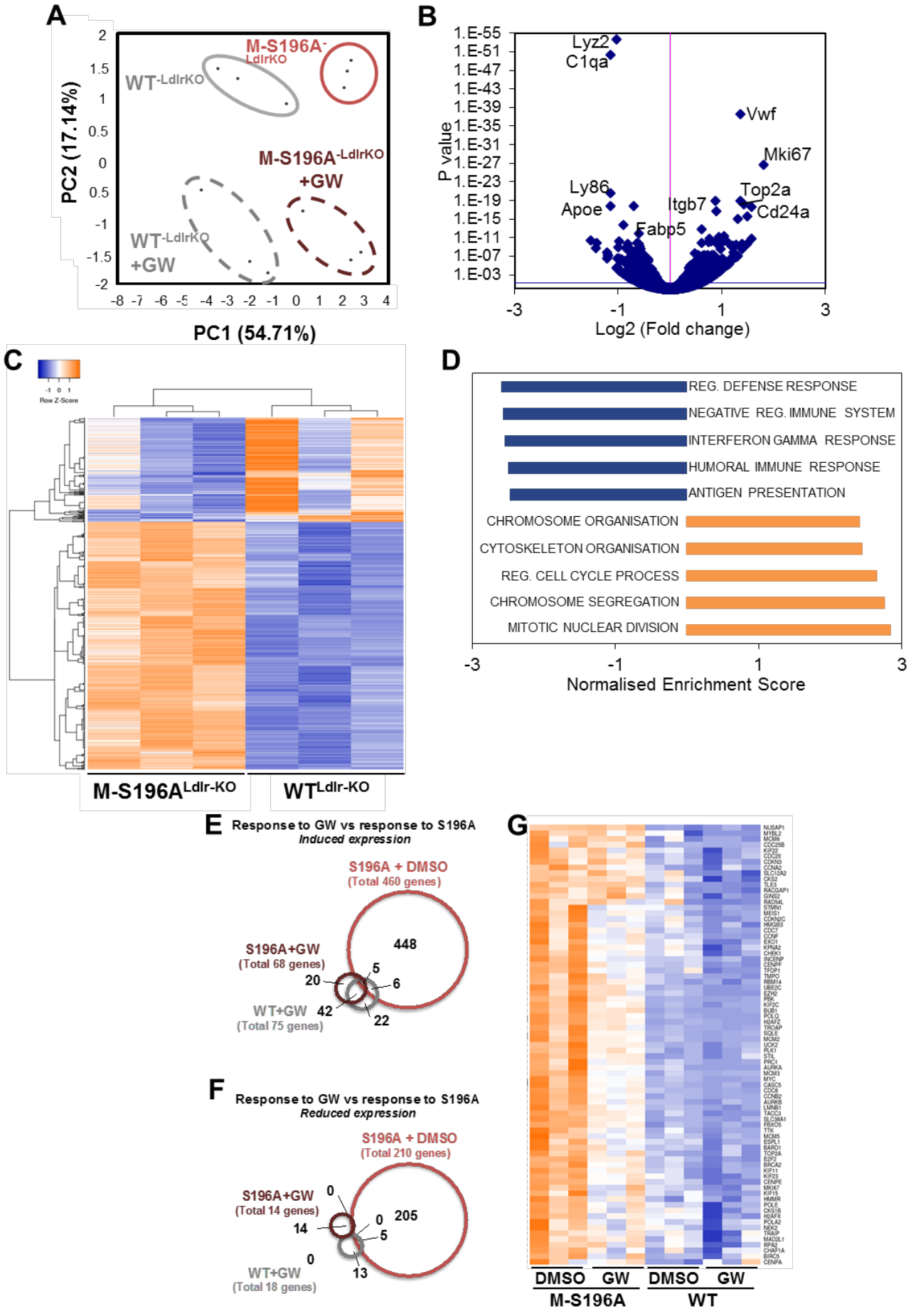

(**A**) Principal Component (PC) Analysis plot showing RNAseq samples from WD-fed mice analysed by genotype and ligand treatment (n=3/group). (**B**) Volcano plot of $\log_2$ ratio vs p-value of differentially expressed genes in GW3965-treated macrophages from WD-fed M-S196A$^{Ldlr\text{-}KO}$ compared to WT$^{Ldlr\text{-}KO}$ mice (n=3/group). Blue line indicates adjusted p-value threshold of 0.04. (**C**) Clustered heatmap of RNAseq gene counts in GW3965-treated macrophages from WD-fed mice (n=3/group) showing genes that exhibit ≥1.3-fold expression, p ≤0.01 over ligand-treated WT$^{Ldlr\text{-}KO}$ cells. (**D**) GSEA analysis showing enriched pathways in M-S196A$^{Ldlr\text{-}KO}$ macrophages incubated with 1μM GW3965 compared to ligand-treated WT$^{Ldlr\text{-}KO}$ cells. (**E, F**) RNAseq analysis on M-S196A$^{Ldlr\text{-}KO}$ and WT$^{Ldlr\text{-}KO}$ macrophages from WD-fed mice exposed to 1μM GW3965 (GW) (n=3/group). Venn diagram of genes (**F**) induced or (**G**) reduced in S196A compared to WT cells. (**G**) Clustered heatmap of RNAseq gene counts of G2M checkpoint genes in macrophages from WD-fed mice (n=3/group).

Supplementary Figure 8

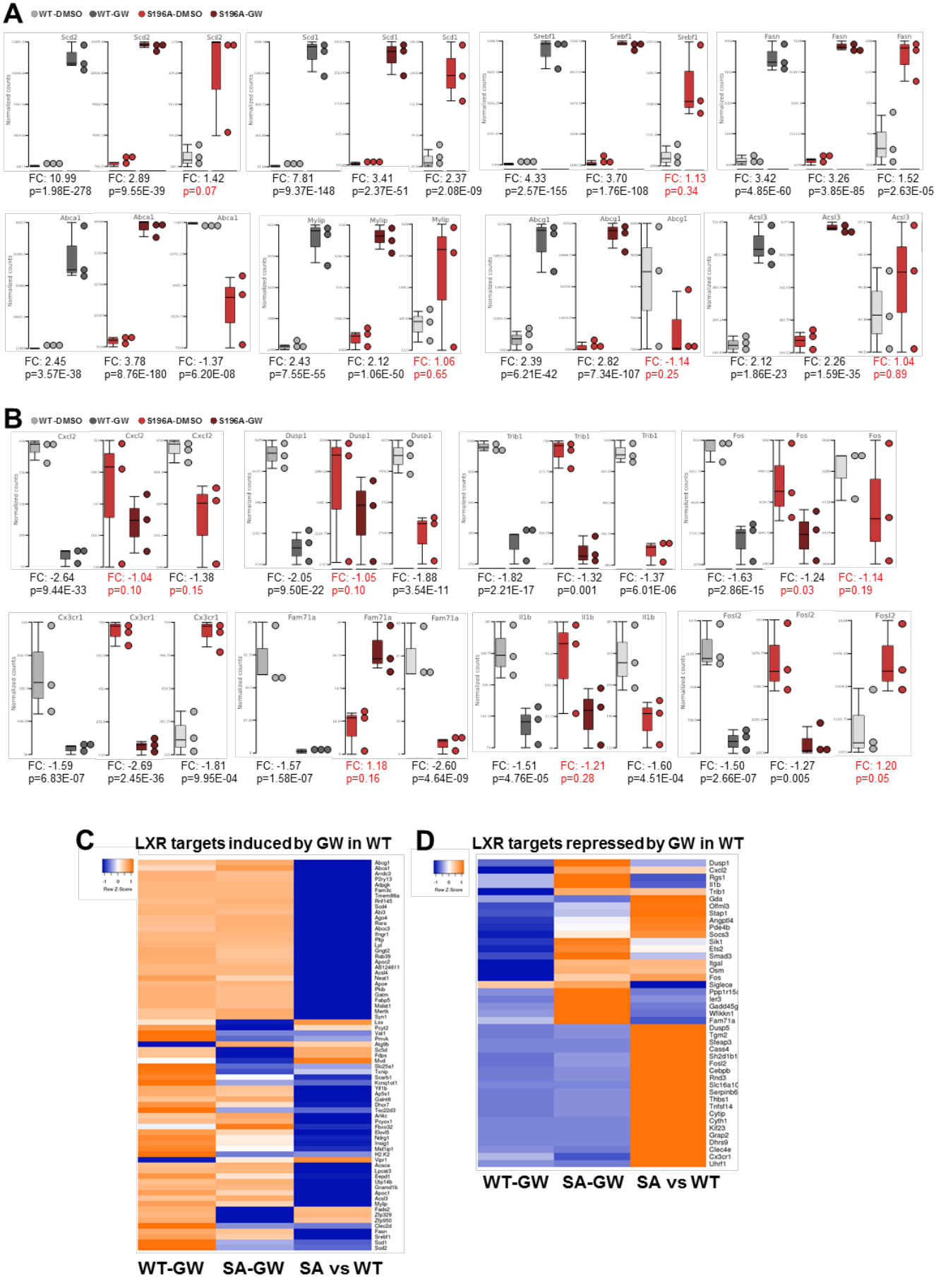

(**A, B**) Combined dot and and box plots depicting normalised RNAseq gene counts showing response to ligand in $WT^{Ldlr\text{-}KO}$ (WT) and M-S196A$^{Ldlr\text{-}KO}$ (S196A) macrophages from WD-fed animals for the top up **(A)** and down **(B)** regulated genes in WT cells. Comparison between DMSO-treated levels between genotypes is also shown. n=3 per genotype or treatment. Fold changes and p values adjusted after FDR 0.05 are shown. Highlighted in red are comparisons that are not statistically significant. (**C, D**) Clustered heatmaps depicting fold changes of all genes significantly (**C**) induced or (**D**) reduced by GW in WT cells (>1.3 fold change, $p< 0.01$), compared to response to GW in S196A, and the expression in S196A vs WT macrophages.

Supplementary Figure 9

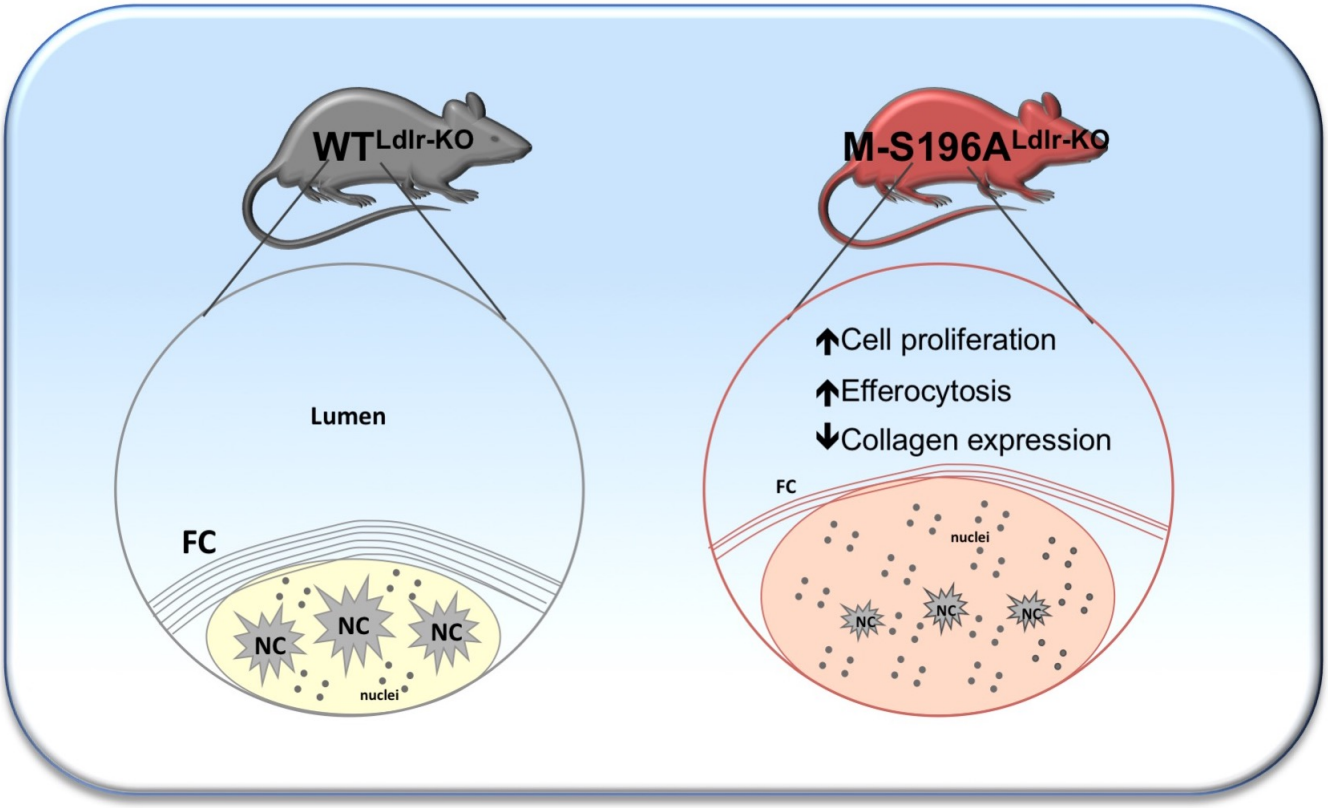

Expression of LXRα-S196A in cells of the myeloid lineage (M-S196A) during the progression of atherosclerosis results in increased atherosclerotic plaque burden associated with plaques that display a distinctive phenotypic profile with (1) increased proliferation of lesion-resident cells, (2) increased apoptotic cell removal by macrophages leading to smaller necrotic cores (NC) and (3) reduced collagen levels and thinner fibrous caps (FC).

Supplementary Figure 10

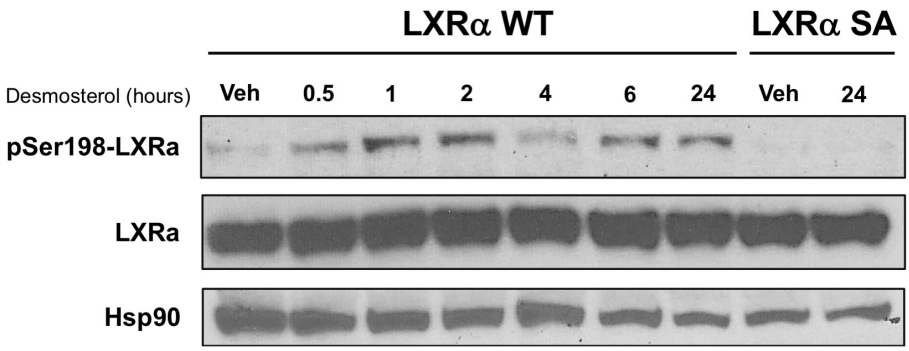

RAW 264.7 cells stably expressing the human LXRα (RAW-hLXRα) or the S198A phospho-mutant (RAW-S198A, equivalent to S196 in the mouse sequence) were incubated with 10 μM Desmosterol or vehicle (Veh) for the indicated periods of time. Nuclear extracts were extracted and phospho-LXRα, total LXRα and Hsp90 were detected by immunoblotting. Shown is a representative experiment of two.

Table S1: Overrepresentation Enrichment Analysis of Reactome Pathways enriched in genes *induced* in S196A

Geneset ID	Name	Gene n	FDR	P
R-MMU-1640170	Cell Cycle	69	0	0
R-MMU-69278	Cell Cycle, Mitotic	57	0	0
R-MMU-68877	Mitotic Prometaphase	23	7.94E-11	1.93E-13
R-MMU-2500257	Resolution of Sister Chromatid Cohesion	22	1.27E-10	4.11E-13
R-MMU-69620	Cell Cycle Checkpoints	29	1.61E-09	6.55E-12
R-MMU-68886	M Phase	30	1.11E-07	5.39E-10
R-MMU-69481	G2/M Checkpoints	22	1.65E-06	9.38E-09
R-MMU-453279	Mitotic G1-G1/S phases	21	1.75E-06	1.14E-08
R-MMU-5663220	RHO GTPases Activate Formins	18	2.72E-06	1.99E-08
R-MMU-68882	Mitotic Anaphase	22	5.39E-06	4.38E-08

Table S2: Overrepresentation Enrichment Analysis of Reactome Pathways enriched in genes *reduced* in S196A

Geneset ID	Name	Gene n	FDR	P
R-MMU-168256	Immune System	43	3.29E-06	2.67E-09
R-MMU-166663	Initial triggering of complement	6	5.81E-06	9.44E-09
R-MMU-3000178	ECM proteoglycans	7	2.49E-05	6.06E-08
R-MMU-166658	Complement cascade	7	3.36E-05	1.09E-07
R-MMU-2022090	Assembly of collagen fibrils	6	7.77E-04	3.16E-06
R-MMU-8948216	Collagen chain trimerization	6	7.84E-04	3.93E-06
R-MMU-1442490	Collagen degradation	7	7.84E-04	4.46E-06
R-MMU-168249	Innate Immune System	29	1.03E-03	6.72E-06
R-MMU-216083	Integrin cell surface interactions	7	1.10E-03	8.03E-06

Table S3: Overrepresentation Enrichment Analysis of Reactome Pathways enriched in genes *induced* in S196A upon GW-activation

Geneset ID	Name	Gene n	FDR	P
R-MMU-1640170	Cell Cycle	35	2.38E-03	1.9E-06
R-MMU-69278	Cell Cycle, Mitotic	29	2.65E-03	4.3E-06
R-MMU-109582	Hemostasis	30	6.36E-03	1.6E-05
R-MMU-2980767	Activation of NIMA Kinases NEK9, NEK6, NEK7	4	6.36E-03	2.1E-05
R-MMU-1538133	G0 and Early G1	6	1.47E-02	6.0E-05
R-MMU-983189	Kinesins	5	2.31E-02	1.1E-04

Table S4: Overrepresentation Enrichment Analysis of Reactome Pathways enriched in genes *reduced* in S196A upon GW-activation

Geneset ID	Name	Gene n	FDR	P
R-MMU-3000178	ECM proteoglycans	6	3.43E-04	6.22E-07
R-MMU-166658	Complement cascade	6	3.43E-04	1.02E-06
R-MMU-2022090	Assembly of collagen fibrils and other multimeric structures	6	3.43E-04	1.28E-06
R-MMU-168256	Immune System	34	3.43E-04	1.39E-06
R-MMU-198933	Immunoregulatory interactions between a Lymphoid and a non-Lymphoid cell	7	2.86E-03	1.60E-05
R-MMU-1474244	Extracellular matrix organization	11	2.86E-03	1.70E-05
R-MMU-216083	Integrin cell surface interactions	6	3.92E-03	3.82E-05
R-MMU-168249	Innate Immune System	24	6.63E-03	8.08E-05
R-MMU-1474228	Degradation of the extracellular matrix	7	7.48E-03	9.72E-05
R-MMU-418594	G alpha (i) signalling events	8	4.59E-02	6.71E-04

Table S5: RT-qPCR primers

Gene	Forward (5' to 3')	Reverse (5' to 3')
Cyclophilin	GGCCGATGACGAGCCC	TGTCTTTGGAACTTTGTCTGCAA
Abca1	GGACATGCACAAGGTCCTGA	CAGAAAATCCTGGAGCTTCAAA
Abcg1	CCTTCCTCAGCATCATGCG	CCGATCCCAATGTGCGA
Srebf1	CAGGAGGACATC TTGCTGCTTC	TTGGGAGGCTGGTTTTGACC
Apoe	CTGACAGGATGCCTAGCCG	CGCAGGTAATCCCAGAGC
Ccr2	GCCATACCTGTAAATGCCATGC	CCAATGCCCTCTTCTGGTCT
Gpr132	TGGCTTGGGTCATTTTAAGC	TCATGGTGGCTCCTATGTGA
Mfge8	GCCTCCCGTTGTTCTACACA	AGACGAGGCGGAAATCTGT
Mertk	GAGCCATCGAGCTTACCTTG	AACTTTGCCGAGAACCAGAA
Gas6	CCGGCTCTGTGACAAAGATG	TTCCTGGTTTGTTGTGGCAG
Foxm1	GAGGTGATCACGGAGACGTT	CTCCTGTCTTTGCCTTGGAG
Ccna2	CTGTCTCTTTACCCGGAGCA	TGTGGTGATTCAAAACTGCCA
Cenpf	GCTTGAAGGACAGCTGGAGA	TCCGCTTTCAACCTTCTGCT
Top2a	GAACATATACTGCTCCGCCC	TTGCTGGGTCACTAACTCCA
Ccnb2	GGCGAAGAAACCTCAGAACA	TCGGCTGCTTGTTGACATTT
Plk1	ATTCCCAAGCACATCAACCC	GGGGTCTGTCTGAAGCATCT
Ccnb1	TGGACTACGACATGGTGCAT	GATGTGCTGCAGAGTTGGTG
Birc5	TGGACAGACAGAGAGCCAAG	CTGCTCAATTGACTGACGGG

Table S6: ChIP-qPCR primers

Gene	Forward (5' to 3')	Reverse (5' to 3')
Abca1	TGAGCTACCCACCCTATGAA CA	CCCCTGAACCCAAGGAAGTG
Srebp1c	TCAGCGAGGCGGCTTTGGA G	CATGTCTTCGATGTCGGTCAG
TULP3	AGATGCTCCACCATACCACA	GCACCCCACCCCAAATAAAG
FoxM1 P1	CCCTGCCTCCTGTCTCATAG	AGAAGGGAGAGCTGCTTTGA
FoxM1 LXRE	GAATCTAGGTGAGGGGCTGG	GATGACTGTGAGCTGCCATG
FoxM1 P2	CCCATCGTCTCTCATCCCTC	TGCCTGCCATTGTGTACTAGA
Top2a P2	CCTGAAGGGGAGCTGATTGT	CCTCAAACCTCAGAGCTCCT
Top2a LXRE2	CGGGAAGGTCAGAAGAAGTC	TGTCCTCACCCATACAGAAGAC
Cenpf LXRE2	TGCAGCTCTCTATACCAAATTCC	ATTTTGTGCCTTTAAACTTCCCA